Hybrid Feedback Path Following for Robotic Walkers via Bang-Bang Control Actions

Marco Andreetto and Stefano Divan and Daniele Fontanelli and Luigi Palopoli

Abstract— **This paper presents a control algorithm conceived to guide a robotic walking assistant along a planned path using electromechanical brakes. The device has been modelled as a Dubins' car, a wheeled vehicle that moves only forward in the plane and constrained by a lower bounded turning radius. In order to reduce the hardware requirements as much as possible, so as to reduce the costs, we work with limited sensory information, so the classic modulated braking guidance cannot be implemented. As a consequence, the vehicle has a very limited set fixed turning radius manoeuvres ruled by a hybrid controller based on three discrete states: go straight, turn right and turn left. Despite of these limitations and in order to ensure a gentle and natural convergence of the user to the planned path, the robot approaches the path with an orientation that depends on its position and that guarantees a continuous curvature of the tracked path. Results are validated using extensive simulations.**

I. INTRODUCTION

The use of robotic platforms to help older adults navigating in complex environments is commonly regarded as an effective means to extend their mobility and, ultimately, to improve their health conditions. The EU Research project ACANTO [1] aims to develop a robotic friend (called *FriWalk*), which offers several types of cognitive and physical support. The *FriWalk* looks no different from a classic rollator, a four wheel cart used to improve stability and receive physical support. The endowed sensing and computing abilities allow the *FriWalk* to understand the environment, localise itself and generate paths that can be followed with safety and comfort. The user is then guided along the path using a Mechanical Guidance Support (MGS).

The MGS utilises electromechanical brakes to steer the vehicle in order to stay as close as possible to the planned path. In this paper, we study a control strategy that fulfils this goal. A few specific issues makes our problem particularly challenging. First, the low target cost of the device prevents us from using expensive sensors to estimate the force and the torque applied by the user to the platform. Second, the use of electromechanical brakes and the sometimes difficult grip conditions make the braking action difficult to modulate. Third, because the guidance system interacts with the user, who ultimately is in charge of the cart motion, the control algorithm should be flexible to adapt to different users and different operating conditions and it should give directions that users should find "sensible" and easy to follow.

The proposed controller reduces the distance from the path by executing "a few" control actions, which are easily understood by the user who can be left in control of her motion for most of the time. A useful inspiration for the proposed controller can be found in the work of Ballucchi et al. [2]. The authors proved that for a vehicle that moves with constant speed and with limited curvature, the control policy that takes the vehicle to the path in minimum time is a bang-bang strategy. For the problem at hand, this means restricting to three control actions: 1. let the user go, 2. force a right turn blocking the right wheel, 3. force a left turn blocking the left wheel. The resulting motion of the vehicle is given by a concatenation of straight lines and circles with fixed radius. The restriction to the bang-bang strategy is convenient because it requires no force measurements and or finely modulated braking actions. However, the minimum time manoeuvres of [2] could appear unnatural and uncomfortable to the user. For this reason, the control strategy derived in this paper adds a degree of freedom in order to specify the *angle of approach* (the angle between the orientation of the vehicle and the tangent to the trajectory). This yields to a continuous curvature of the tracked path, which has been proved in [3], [4] to be the natural walking way of humans.

The paper is organised as follows. In Section II we offer a quick survey of the related work. In Section III we introduce the most important definitions and state the problem in formal terms. In Section IV, we describe our control strategy and in Section V we extend it to varying approaching angles. Section VI shows its performance by means of simulations. In Section VII we state our conclusions and announce future work directions.

II. RELATED WORK

The device adopted in this paper can be modelled as a particular Dubins' car with a fixed curvature radius. One notable solution that steers a Dubins' car along a given path has been introduced by [2]. The proposed solution is based on a discontinuous control scheme on the angular velocity of the vehicle. This approach has been further developed in [5] for optimal route tracking control minimising the approaching path length. The optimal problem is based on the definition of a switching logic that determines the appropriate state of a hybrid system. From the same authors, an optimal controller able to track generic paths that are

This project has received funding from the European Unions Horizon 2020 Research and Innovation Programme - Societal Challenge 1 (DG CONNECT/H) under grant agreement n° 643644 "ACANTO - A CyberphysicAl social NeTwOrk using robot friends".

D. Fontanelli is with the Department of Industrial Engineering (DII), University of Trento, Via Sommarive 5, Trento, Italy daniele.fontanelli@unitn.it. S. Divan and L. Palopoli are with the Department of Information Engineering and Computer Science (DISI), University of Trento, Via Sommarive 5, Trento, Italy {palopoli,divan,andreetto}@disi.unitn.it

unknown upfront, provided some constraints on the path curvature are satisfied, has been presented in [6]. This second solution considers the curvature of the path as a disturbance which has to be rejected.

For what concerns assistive carts, the passive walker proposed by Hirata [7] is a standard walker, with two caster wheels and a pair of electromagnetic brakes mounted on fixed rear wheels, which is essentially the same configurations that we consider in this paper. The authors propose a guidance solution using differential braking, which is inspired to many stability control systems for cars [8]. By suitably modulating the braking torque applied to each wheel, the walker is steered toward a desired path [9].

The walking assistant considered in this paper builds atop the model proposed in [7], [9]. In our previous work [10], we proposed a control algorithm based on the solution of an optimisation problem which minimises the braking torque. However, the control law relies on real–time measurements of the torques applied to the walker, which are difficult without expensive sensors. For example, the *i-Walker* rollator [11] is equipped with triaxial force sensors on the handles to estimate the user applied forces. Nevertheless, its cost is on the order of some thousands euros, which makes it unaffordable for the majority of the potential users. Therefore, to limit the system cost and simplify the algorithm design, we restrict the possible actions to turn left or right by blocking alternatively the left or right wheel, thus casting the problem to the class of path following problems for nonholonomic vehicles with limited curvature radius. In light of this choice, this paper represents a first attempt to fuse hybrid control laws conceived for optimal tracking of unicycle-like vehicles [6] with the nonlinear trajectory tracking approaches proposed, for instance, in [12], [13]. To this end, we first generalise the hybrid control law proposed in [6] to desired angles of approach to the reference path. This degree of freedom can be used to ensure an approaching route with continuous curvature, greatly improving the user comfort, according to the results of [3], [4]. Other possible uses of the customisation are obstacles avoidance and minimum time approaches.

III. Background and Problem Formulation

The device considered in this paper is derived from a commercial walker endowed with electro-mechanical brakes on the rear wheels along with other mechatronic components. The *FriWalk* localisation is based on incremental encoders mounted on the rear wheels, on an inertial platform measuring the vehicle accelerations and angular velocities, and on exteroceptive sensors, such as RFID readers and cameras. The vehicle uses vision technologies to detect information on the surrounding environment and to plan the safest course of action for the user [14], [15]. Due to the described abilities, the reference path is assumed to be known up-front and its localisation is considered solved by means of the solution presented in [16], [17].

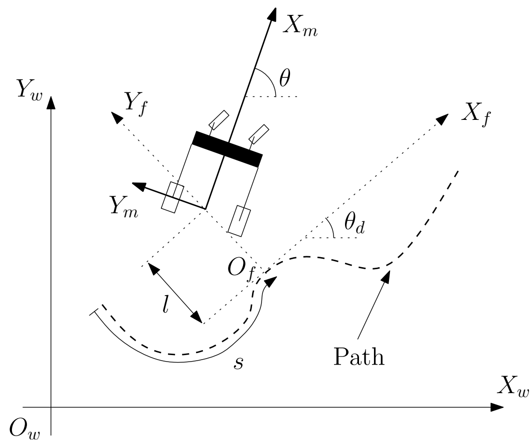

Fig. 1. Vehicle to path configuration and reference frames.

A. Vehicle Model

With reference to Fig. 1, let $\langle W \rangle = \{O_w, X_w, Y_w, Z_w\}$ be a fixed right-handed reference frame, whose plane $\Pi = X_w \times Y_w$ is the plane of motion of the cart, Z_w pointing outwards the plane Π and let O_w be the origin of the reference frame.

Let $\mathbf{x} = [x,\, y,\, \theta]^T \in \mathbb{R}^2 \times S$ be the kinematic configuration of the cart, where $(x,\, y)$ are the coordinates of the mid–point of the rear wheels axle in Π and θ is the orientation of the vehicle w.r.t. the X_w axis (see Fig. 1). The dynamic model of the *FriWalk* can be assimilated to a unicycle

$$\begin{bmatrix} \dot{x} \\ \dot{y} \\ \dot{\theta} \end{bmatrix} = \begin{bmatrix} v\cos(\theta) \\ v\sin(\theta) \\ \omega \end{bmatrix} \Leftrightarrow \begin{bmatrix} \dot{s} \\ \dot{l} \\ \dot{\tilde{\theta}} \end{bmatrix} = \begin{bmatrix} v\cos(\tilde{\theta})/(1-c(s)l) \\ v\sin(\tilde{\theta}) \\ \tilde{\omega} \end{bmatrix} \quad (1)$$

where v is the forward velocity of the vehicle and ω its angular velocity. s is the curvilinear abscissa along the path, l is the distance between the origin of the Frenet frame $\langle F \rangle$ and the reference point of the *FriWalk* along the Y-axis of the Frenet frame, and θ_d is the angle between the X_w-axis and the X-axis of the Frenet frame[1] (see Fig. 1). Therefore, $\tilde{\theta} = \theta - \theta_d$ and $\tilde{\omega} = \dot{\tilde{\theta}} = \omega - c(s)\dot{s}$. Furthermore, the path curvature is defined as $c(s) = d\theta_d(s)/ds$. It is worthwhile to note that the models (1) are commonplace in the literature and can be found, for example, in [18], [19], [12].

As aforementioned, the considered vehicle is passive, i.e. the forward velocity v is imposed by the user, while the angular velocity is modified by both the torque applied by the user to the cart and the torque applied by the braking system[2]. By direct experimental measurements made on the system at hand, we have observed that the torques applied by the user to the mechanical system are negligible with respect to the maximum braking action. Moreover, the inertia of the system as well as the maximum forward velocity v are limited. As a consequence, the time needed to stop the wheel rotation

[1] The Frenet frame is centred in the closest point of the path to the vehicle, and it has its x–axis tangent to the path.

[2] Actually, the braking system acts on the real wheels. The torque applied to the cart is a linear combination of the toques applied to the wheels [20].

is negligible. In light of the description given previously, if the brake is fully active on the right wheel, the vehicle will end-up in following a circular path with fixed curvature radius $R = d/2$, where d is the rear wheel inter-axle length, travelled in clockwise direction if $v > 0$ (counter-clockwise for $v < 0$). The circular path with the same radius R will be instead followed in counter-clockwise direction if the left brake is fully active and $v > 0$ (clockwise for $v < 0$). As a consequence, in all the cases of active braking system, $|\omega| = |v|/R$. If no braking action is applied at all, the user will drive the *FriWalk* uncontrolled. From a control perspective, the previous model turns into a nonholonomic nonlinear vehicle with limited curvature and quantised inputs: turn left, turn right, move freely.

B. Problem Formulation

We require the walker to converge to our planned path defined in Π, which we will assume to be smooth (i.e., with a well defined tangent on each point) and with a known curvature. The planned path is typically composed of *clothoids*, in particular straight segments and circular arcs. With reference to (1), the problem to solve is formalised as follows:

$$\lim_{t \to +\infty} l(t) = 0, \quad \text{and} \quad \lim_{t \to +\infty} \tilde{\theta}(t) = 0. \tag{2}$$

In general, the path following problem requires the design of a control law $v(t)$ and $\omega(t)$ for the system in (1) that makes the origin $(l, \tilde{\theta})$ *global attractive*. In our case, $v > 0$ is imposed by the user, then it is not a control input but a given parameter, while $\omega(t)$ can assume three values only: $\omega = 0$ (free walk), $\omega = +v/R$ (block left wheel, hence turn left), $\omega = -v/R$ (block right wheel, hence turn right).

IV. Path Following Algorithm

The first part of the solution proposed in this paper relies on the hybrid automaton designed in [6], which proposes a minimum length trajectory to reach a desired path for limited curvature unicycle-like vehicles. This solution is based on a hybrid feedback controller solving (2) for unicycle-like vehicles with bounded curvature radius. The authors show that their hybrid controller is stable with respect to the path-related coordinates $(\tilde{l}, \tilde{\theta})$, where $\tilde{l} = l/R$ and R is the fixed minimum turning radius of the vehicle. As aforementioned, the controller automaton comprises three different manoeuvres, i.e., *Go Straight*, *Turn Right* and *Turn Left*, which are defined in terms of the angular velocity ω of (1) as

$$\begin{cases} \omega = 0, & \text{if } \textit{Go Straight}, \\ \omega = -\frac{v}{R}, & \text{if } \textit{Turn Right}, \\ \omega = \frac{v}{R}, & \text{if } \textit{Turn Left}, \end{cases} \tag{3}$$

assuming the forward input $v > 0$ is known.

The hybrid automaton comprises three states, in which the three manoeuvres are coded according to the state of the vehicle. To this end, the state space $(\tilde{l}, \tilde{\theta})$ is suitably partitioned into a set of non-overlapping regions. In each region only one of the three manoeuvres is active. In order to define these regions for our purposes, let us generalise the boundary functions reported in [6] as:

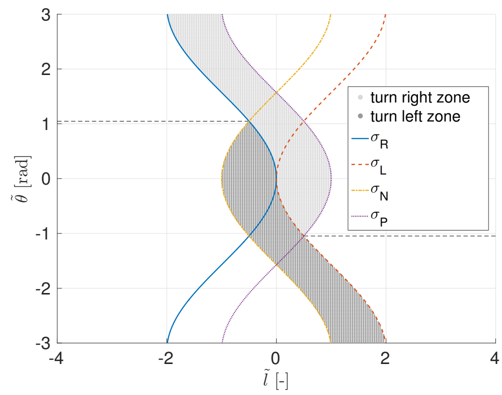

Fig. 2. Boundary functions and state space partition induced by the boundary function for $\delta = -\text{sing}(\tilde{l})\pi/3$.

$$\begin{aligned} \sigma_R(\tilde{l}, \tilde{\theta}) &= \tilde{l} + 1 - \cos(\tilde{\theta}), \\ \sigma_L(\tilde{l}, \tilde{\theta}) &= \tilde{l} - 1 + \cos(\tilde{\theta}), \\ \sigma_N(\tilde{l}, \tilde{\theta}, \delta) &= \tilde{l} + 1 - 2\cos(\delta) + \cos(\tilde{\theta}), \\ \sigma_P(\tilde{l}, \tilde{\theta}, \delta) &= \tilde{l} - 1 + 2\cos(\delta) - \cos(\tilde{\theta}), \end{aligned} \tag{4}$$

where δ is the approaching angle, i.e., the desired orientation by which the vehicle approaches the path. An example of these boundary functions is visible in Figure 2. The regions defined in (4) coincide with the regions of [6] by imposing $\delta = -\text{sign}(\tilde{l})\frac{\pi}{2}$ (minimum time approach). Given the current state $(\tilde{l}, \tilde{\theta})$, the control action for the modified regions are:

- if $(\tilde{l}, \tilde{\theta}) \in (\sigma_P > 0 \ \wedge \ \tilde{\theta} \geq \delta) \ \vee \ (\sigma_L > 0 \ \wedge \ \tilde{\theta} \leq \delta)$, then
$$\begin{cases} \tilde{\theta} = \delta & \Rightarrow \ \textit{Go Straight}, \\ \tilde{\theta} > \delta \ \wedge \ \tilde{\theta} < \pi + \delta & \Rightarrow \ \textit{Turn Right}, \\ \text{otherwise} & \Rightarrow \ \textit{Turn Left}; \end{cases}$$
- if $(\tilde{l}, \tilde{\theta}) \in (\sigma_R < 0 \ \wedge \ \tilde{\theta} \geq \delta) \ \vee \ (\sigma_N < 0 \ \wedge \ \tilde{\theta} \leq \delta)$, then
$$\begin{cases} \tilde{\theta} = \delta & \Rightarrow \ \textit{Go Straight}, \\ \tilde{\theta} < \delta \ \wedge \ \tilde{\theta} > -\pi + \delta & \Rightarrow \ \textit{Turn Left}, \\ \text{otherwise} & \Rightarrow \ \textit{Turn Right}; \end{cases}$$
- if $(\tilde{l}, \tilde{\theta}) \in (\sigma_P \leq 0 \ \wedge \ \sigma_R \geq 0 \ \wedge \ \tilde{\theta} \geq 0) \ \vee \ (\sigma_L > 0 \ \wedge \ \sigma_P \leq 0 \ \wedge \ \tilde{\theta} < 0)$, then *Turn Right*;
- if $(\tilde{l}, \tilde{\theta}) \in (\sigma_N \geq 0 \ \wedge \ \sigma_L \leq 0 \ \wedge \ \tilde{\theta} \leq 0) \ \vee \ (\sigma_N \geq 0 \ \wedge \ \sigma_R < 0 \ \wedge \ \tilde{\theta} > 0)$, then *Turn Left*.

Notice that the described procedure can be interpreted as a state feedback $\omega = g(\tilde{l}, \tilde{\theta})$ once δ is chosen as a function of the state $(\tilde{l}, \tilde{\theta})$, i.e. $\delta = \delta(\tilde{l}, \tilde{\theta})$. The trajectories in the phase portrait of Figure 3 are obtained by applying only one of the actions (3).

By switching among the different manoeuvres in (3) using the boundary regions defined by (4), complex trajectories can be obtained, as reported in Figure 4. The trajectories A and D are obtained when the vehicle reaches the path

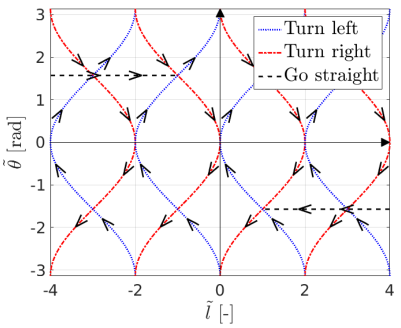

Fig. 3. Complete *Turn Right* (solid lines) and *Turn Left* (dash dotted line) manoeuvres originating from positions $\tilde{l} = \{-4, -2, 0, 2, 4\}$. The dashed line corresponds to the *Go Straight* manoeuvre for a choice of $\delta = -\text{sign}(\tilde{l})\pi/2$.

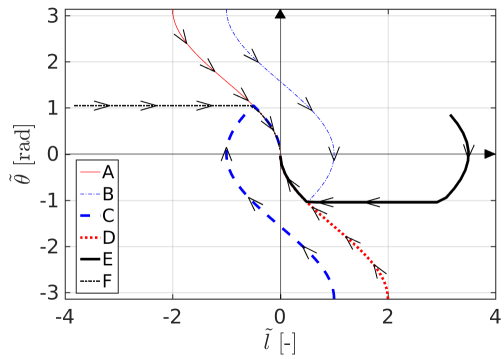

Fig. 4. Phase portrait for 6 different manoeuvres (named *A*, *B*, *C*, *D*, *E* and *F* and detailed in the text) of the generalised hybrid controller defined in (4) for $\delta = -\text{sing}(\tilde{l})\pi/3$.

(according to (2)) with a single manoeuvre (*Turn Right* for *A* and *Turn Left* for *D*, see also Figure 3). In the trajectories *B* and *C* the robot reaches the path with two manoeuvres: first a *Turn Left* and then a *Turn Right* in the case of *B*; the converse happens for trajectory *C*. The trajectory *E* is obtained when the robot starts far from the path ($\tilde{l} > 1$) and with an orientation $\tilde{\theta} \in [-\delta, \pi - \delta]$. The first part of the manoeuvre is obtained by a *Turn Right* with minimum radius curvature until it is oriented towards the path to reach (a linear segment in this example), with $\tilde{\theta} = -\delta$. Then the robot proceeds towards the path performing a *Go Straight* manoeuvre and, finally, it rotates performing a final *Turn Left* manoeuvre. Notice that this is the maximum sequence of manoeuvres to converge to the path from any initial position. In the trajectory *F* the robot starts far from the path but with the desired orientation $\tilde{\theta} = \delta$, therefore it first goes straight with a *Go Straight* manoeuvre and then switches to the *Turn Right* mode to lie exactly on the path.

Once the robot reaches the path with the correct orientation, it permanently remains there by means of a set of zero-length manoeuvres (chattering phenomenon) ruled again by the boundary regions (4) and providing that the path curvature is feasible according to the minimum curvature radius constraint $\max_s |c(s)| \leq \frac{1}{R}$, i.e., a path whose maximum curvature $c(s)$ does not exceed the inverse of the turning radius of the vehicle. The convergence property is ensured by proper choices of δ as a function of the normalised distance from the path $\tilde{l}$, as formalised in what follows.

Theorem 1: Given the feedback controller defined by the boundary regions (4), a path satisfying $\max_s |c(s)| \leq \frac{1}{R}$ and the approaching angle $\delta(\tilde{l}) = -\frac{\pi}{2}\,\text{sign}(\tilde{l})$, the origin of the space $(\tilde{l}, \tilde{\theta})$ is almost globally attractive.

The proof of Theorem 1 directly comes from [6] for the particular choice $\delta(\tilde{l}) = -\frac{\pi}{2}\,\text{sign}(\tilde{l})$. Notice that since $\dot{s}$ is singular for $lc(s) = 1$ in (1), the result of Theorem 1 proves *almost* global attractiveness for the pair $(l, \tilde{\theta})$. The singularity can be solved by introducing an auxiliary control input governing the motion of the Frenet frame along the path [12].

It is worthwhile to recall that, in order to follow a path with generic curvature $\max_s |c(s)| \leq \frac{1}{R}$, continuous switches between the inputs (3) imposed by the controller are required (chattering phenomenon).

V. Varying Approaching Angle

The solution presented in Section IV ensures the convergence to the desired path within a maximum of three manoeuvres (see the trajectory *E* in Figure 4). This produces an approaching route made by straight lines and arcs of circle, that is discontinuous in the curvature. These curvature jumps, induced by the discontinuous function $\delta(\tilde{l})$, highly differ from the natural human walking. In fact, in [3] it is shown that the human motion minimises exactly the variation of the curvature. To produce an approaching route that is continuous in the curvature, the function $\delta(\tilde{l})$ has to be continuous as well. Geometrically, if $|\delta(\tilde{l})|$ varies, the vehicle tends towards the desired path by following an *approaching path*, i.e. a second path that joints the initial vehicle position with the desired path. Since the approaching path can be interpreted as a path following per-se, it can be followed by means of chattering among the inputs (3), providing that its maximum curvature does not exceed R^{-1}, as stated previously. The following theorem shows the convergence in the sense of (2) in the case of the quantised inputs (3) with fixed curvature radius for a generic continuous odd function $\delta(\tilde{l})$. The proof extends and subsumes the results in [12], where the convergence was granted for a standard unicycle–like vehicle, i.e., continuous inputs and no bounded curvature.

Theorem 2: For any function $\delta(\tilde{l})$ continuous, monotonic, limited $|\delta(\tilde{l})| \in (0, \frac{\pi}{2}]$, odd and negative in the second quadrant (i.e. with $-\text{sign}(\tilde{l})\frac{\partial \delta(\tilde{l})}{\partial \tilde{l}} \geq 0$ and $\tilde{l}\delta(\tilde{l}) > 0$), the origin of the space $(\tilde{l}, \tilde{\theta})$ is almost globally attractive.

Proof: Let us consider a $\delta(\tilde{l})$ that satisfies the hypotheses (e.g., $\delta(\tilde{l}) = -\frac{\pi}{2}\tanh(\tilde{l})$ depicted with a dashed line in Figure 5). Whenever the vehicle is in a configuration $\tilde{\theta} \neq \delta(\tilde{l})$, either it steers on the left or on the right according to the boundary regions (4). By the property of $\delta(\tilde{l})$, it follows immediately that the turning manoeuvre intersects $\delta(\tilde{l})$, thus reaching in finite time $\tilde{\theta} = \delta(\tilde{l})$ (Figure 5).

From this point on, if $|\dot{\delta}(\tilde{l})| \leq v/R$, $\forall \tilde{l}$, i.e., the commanded $\delta(\tilde{l})$ has instantaneous curvatures that are less than

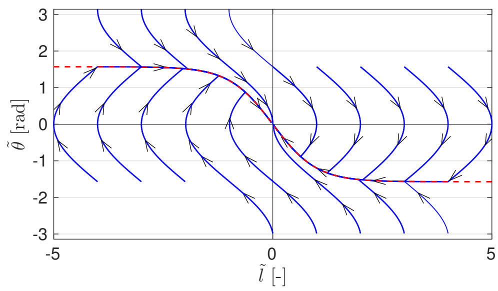

Fig. 5. Phase portrait (solid lines) from various initial vehicle configurations when $\delta(\tilde{l}) = -\frac{\pi}{2}\tanh(\tilde{l})$ (dashed line) is a feasible reference angle.

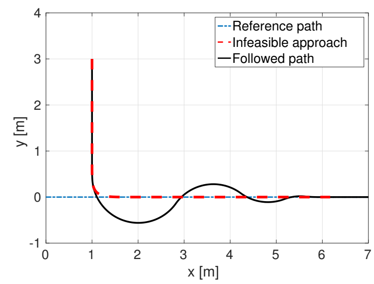

(a)

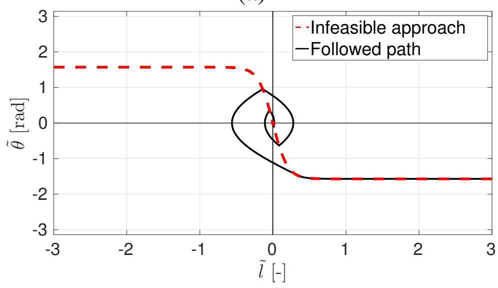

(b)

Fig. 6. Vehicle trajectory (solid line) in the plane of motion (a) and in the phase portrait (b) for an infeasible reference angle $\delta(\tilde{l})$ (dashed line). The reference trajectory is depicted with a dash–dotted line.

R^{-1}, the vehicle remains on the graph of $\tilde{\theta} = \delta(\tilde{l})$ using a chattering approach. The convergence to the origin $(\tilde{l}, \tilde{\theta}) = (0, 0)$ is then guaranteed by [12].

However, it may happen that $|\dot{\delta}(\tilde{l})| > v/R$ (for example, due to the path curvature changes). In such a case, the reference of $\delta(\tilde{l})$ is infeasible for the limited turning radius vehicle. Let us define with $\bar{t}$ the time in which the vehicle departs from the condition $\tilde{\theta} = \delta(\tilde{l})$ due to the limited turning radius R. Using the previous arguments, the hybrid controller will steer the vehicle on the right or on the left to reach again $\tilde{\theta} = \delta(\tilde{l})$, say at time $\hat{t}$. From the symmetry with respect to the $\tilde{\theta} = 0$ axis of the turning manoeuvres (see Figure 3), it follows immediately that $|\tilde{\theta}(\hat{t})| < |\tilde{\theta}(\bar{t})|$ (see Figure 6). Since the condition $\tilde{\theta} = \delta(\tilde{l})$ and $\tilde{\theta} = 0$ implies $\tilde{l} = 0$, the attractiveness of the origin is proved. ■

Remark 1: The result of Theorem 2 still holds for non-odd functions. However, the theorem is presented in this form to simplify the analysis and clarify the extension to quantised inputs of the results in [12]. Moreover, the theorem is still valid for time varying δ functions.

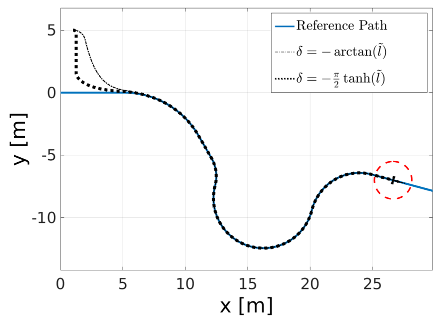

Fig. 7. Examples of vehicle trajectories using $\delta(\tilde{l}) = -\frac{\pi}{2}\tanh(\tilde{l})$ (thick dotted line) and $\delta(\tilde{l}) = -\arctan(\tilde{l})$ (thin dotted line) controlled towards a generic reference path (solid line).

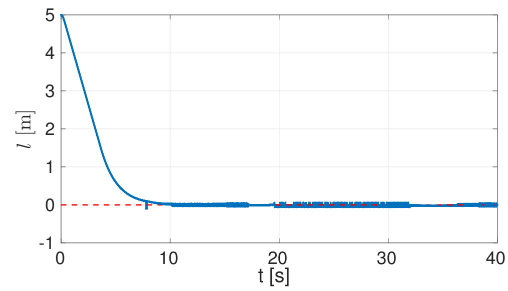

(a)

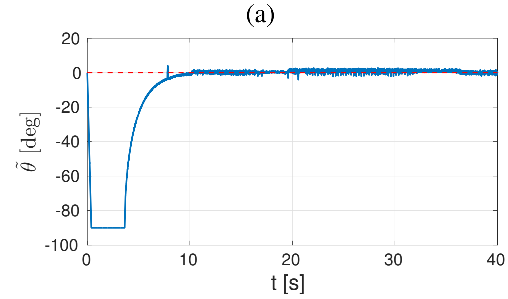

(b)

Fig. 8. Time evolution of the variables l (a) and $\tilde{\theta}$ (b) for the trajectory generated assuming $\delta(\tilde{l}) = -\frac{\pi}{2}\tanh(\tilde{l})$ and depicted in Figure 7.

VI. Simulations Results

To show the effectiveness of the proposed solution, simulations are reported for a generic path. Figure 7 reports the trajectory followed by the vehicle starting with an initial configuration $(x, y, \theta) = (1, 5, 0)$ and following a generic reference path. The forward velocity is imposed equal to a dummy value of $v = 1$ m/s. The path position reached by the robot after 40 s is highlighted with a dashed circle. Two functions $\delta(\tilde{l}) = -\frac{\pi}{2}\tanh(\tilde{l})$ and $\delta(\tilde{l}) = -\arctan(\tilde{l})$ are adopted for comparison. The corresponding distance to the path l and relative angle $\tilde{\theta}$ are reported in Figure 8 for $\delta(\tilde{l}) = -\frac{\pi}{2}\tanh(\tilde{l})$. The high frequency oscillations are due to the continuous switching between the three manoeuvres (3), which is necessary to follow a path with generic curvature (chattering phenomenon).

In order to evaluate the comfort for the user, we consider the cost function

$$J = \int_0^T \left(v^2(\tau) + \kappa^2(\tau)\right) d\tau, \quad (5)$$

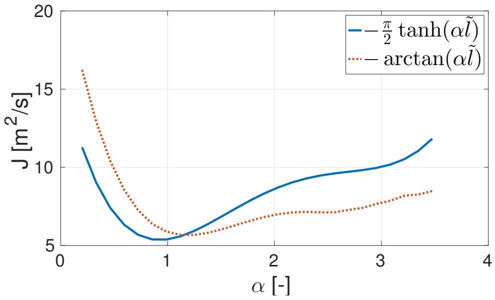

Fig. 9. Cost function J in (5) computed with two different $\delta(\tilde{l})$ functions.

where T is the time in which the path is reached and $\kappa(t) = \dot{c}(s(t))$ is the time derivative of the curvature. In [3] it is observed that a human naturally minimises the cost function (5) during her motion. We evaluate the cost J using the two approaching angles presented previously, i.e., $\delta(\tilde{l}) = -\frac{\pi}{2}\tanh(\alpha\tilde{l})$ and $\delta(\tilde{l}) = -\arctan(\alpha\tilde{l})$. $\alpha > 0$ is a parameter governing the feasibility of the approaching path: increasing the value of α, the approaching path becomes unfeasible (see Figure 6). To properly evaluate the behaviour of the proposed control law, the vehicle is controlled on a simple linear path starting from a fixed distance $l(0)$ and orientation $\theta(0) = -\frac{\pi}{2}\tanh(\alpha\tilde{l}(0))$ for the first case, while $\theta(0) = -\arctan(\alpha\tilde{l}(0))$ for the second case. This way, the vehicle is oriented in the initial position with the approaching angle, i.e. $\tilde{\theta}(0) = \delta(\tilde{l}(0))$. The value of κ is obtained by a stable numeric derivative, while is again fixed to a dummy $v = 1$ m/s. Figure 9 shows that J is minimised, i.e., the comfort is maximised, for $\alpha \approx 1$ for both the approaching functions. Moreover, it is clearly visible how the user comfort is reduced if α decreases, because the convergence to the path is too long. Similarly, if α is too large, the comfort again decreases because the reference $\delta(\tilde{l})$ becomes unfeasible and, hence, a number of correcting manoeuvres are needed (see Figure 6). Finally, it is important to remark that the solution with constant δ returns a value of J that is much higher (theoretically infinite) than those depicted in Figure 9, thus confirming the validity of the proposed solution.

VII. Conclusions

In this paper we have presented a passive control strategy for a robotic walking assistant that guides a senior user with mobility problems along a planned path. The control strategy exploits the electromechanical brakes mounted on the rear wheels of the walker. Due to cost limits, the solution proposed is based on a simple actuation strategy in which the braking system is controlled with a bang-bang control. We show that it is possible to secure a gentle and natural (continuous in curvature) convergence to the path by extending to quantised inputs known results in the literature.

Future developments will aim at implementing the proposed solution on the *FriWalk* and to extend the result presented to a broader class of nonholonomic vehicles. A preliminary study to face the chattering phenomenon can be found in [21].

References

[1] "ACANTO: A CyberphysicAl social NeTwOrk using robot friends," http://www.ict-acanto.eu/acanto, February 2015, EU Project.

[2] A. Balluchi, A. Bicchi, A. Balestrino, and G. Casalino, "Path tracking control for dubin's cars," in *Proc. IEEE Conf. on Robotics and Automation (ICRA)*, vol. 4, Apr 1996, pp. 3123–3128.

[3] G. Arechavaleta, J. P. Laumond, H. Hicheur, and A. Berthoz, "An optimality principle governing human walking," *IEEE Transactions on Robotics*, vol. 24, no. 1, pp. 5–14, Feb 2008.

[4] K. Mombaur, A. Truong, and J.-P. Laumond, "From human to humanoid locomotionan inverse optimal control approach," *Autonomous robots*, vol. 28, no. 3, pp. 369–383, 2010.

[5] P. Soueres, A. Balluchi, and A. Bicchi, "Optimal feedback control for route tracking with a bounded-curvature vehicle," *International Journal of Control*, vol. 74, no. 10, pp. 1009–1019, 2001.

[6] A. Balluchi, A. Bicchi, and P. Soueres, "Path-following with a bounded-curvature vehicle: a hybrid control approach," *International Journal of Control*, vol. 78, no. 15, pp. 1228–1247, 2005.

[7] Y. Hirata, A. Hara, and K. Kosuge, "Motion control of passive intelligent walker using servo brakes," *IEEE Transactions on Robotics*, vol. 23, no. 5, pp. 981–990, 2007.

[8] T. Pilutti, G. Ulsoy, and D. Hrovat, "Vehicle steering intervention through differential braking," in *Proceedings of the 1995 American Control Conference*, vol. 3, 1995, pp. 1667–1671.

[9] M. Saida, Y. Hirata, and K. Kosuge, "Development of passive type double wheel caster unit based on analysis of feasible braking force and moment set," in *Proceedings of the 2011 IEEE/RSJ International Conference on Intelligent Robots and Systems*, 2011, pp. 311–317.

[10] D. Fontanelli, A. Giannitrapani, L. Palopoli, and D. Prattichizzo, "A Passive Guidance System for a Robotic Walking Assistant using Brakes," in *Proc. IEEE Int. Conf. on Decision and Control (CDC)*. Osaka, Japan: IEEE, 15-18 Dec. 2015, pp. 829–834.

[11] U. Cortes, C. Barrue, A. B. Martinez, C. Urdiales, F. Campana, R. Annicchiarico, and C. Caltagirone, "Assistive technologies for the new generation of senior citizens: the share-it approach," *International Journal of Computers in Healthcare*, vol. 1, no. 1, pp. 35–65, 2010.

[12] D. Soetanto, L. Lapierre, and A. Pascoal, "Adaptive, non-singular path-following control of dynamic wheeled robots," in *IEEE Conf. on Decision and Control*, vol. 2. IEEE, 2003, pp. 1765–1770.

[13] Z.-P. Jiang, E. Lefeber, and H. Nijmeijer, "Saturated stabilization and tracking of a nonholonomic mobile robot," *Systems & Control Letters*, vol. 42, no. 5, pp. 327–332, 2001.

[14] A. Colombo, D. Fontanelli, A. Legay, L. Palopoli, and S. Sedwards, "Motion planning in crowds using statistical model checking to enhance the social force model," in *Decision and Control (CDC), 2013 IEEE 52nd Annual Conference on*. IEEE, 2013, pp. 3602–3608.

[15] ——, "Efficient customisable dynamic motion planning for assistive robots in complex human environments," *Journal of Ambient Intelligence and Smart Environments*, vol. 7, no. 5, pp. 617–633, 2015.

[16] P. Nazemzadeh, D. Fontanelli, D. Macii, T. Rizano, and L. Palopoli, "Design and Performance Analysis of an Indoor Position Tracking Technique for Smart Rollators," in *International Conference on Indoor Positioning and Indoor Navigation (IPIN)*. Montbeliard, France: IEEE GRSS, 28-31 Oct. 2013, pp. 1–10.

[17] P. Nazemzadeh, F. Moro, D. Fontanelli, D. Macii, and L. Palopoli, "Indoor Positioning of a Robotic Walking Assistant for Large Public Environments," *IEEE Trans. on Instrumentation and Measurement*, vol. 64, no. 11, pp. 2965–2976, Nov 2015.

[18] A. De Luca, G. Oriolo, and C. Samson, "Feedback control of a nonholonomic car-like robot," in *Robot motion planning and control*. Springer, 1998, pp. 171–253.

[19] L. Lapierre and D. Soetanto, "Nonlinear path-following control of an AUV," *Ocean engineering*, vol. 34, no. 11, pp. 1734–1744, 2007.

[20] D. Fontanelli, A. Giannitrapani, L. Palopoli, and D. Prattichizzo, "Unicycle Steering by Brakes: a Passive Guidance Support for an Assistive Cart," in *Proc. IEEE Int. Conf. on Decision and Control*. Florence, Italy: IEEE, 10-13 Dec. 2013, pp. 2275–2280.

[21] M. Andreetto, S. Divan, D. Fontanelli, and L. Palopoli, "Passive Robotic Walker Path Following with Bang-Bang Hybrid Control Paradigm," in *Proceedings of the IEEE/RSJ International Conference on Intelligent Robots and Systems*. Seoul, South Korea: IEEE, 2016, accepted.